Visual Neuroscience (2004), **21**, 703–713. Printed in the USA.

DOI: 10.1017/S0952523804045055

Functionally intact glutamate-mediated signaling in bipolar cells of the TRKB knockout mouse retina

BAERBEL ROHRER,[1,2] ROMAN BLANCO,[3] ROBERT E. MARC,[4] MARCIA B. LLOYD,[5] DEAN BOK,[5] DAVID M. SCHNEEWEIS,[6] AND LOUIS F. REICHARDT[7]

[1]Department of Ophthalmology, Medical University of South Carolina, Charlston
[2]Department of Physiology and Neuroscience, Medical University of South Carolina, Charleston
[3]Department of Ophthalmology, Universidad Autonoma of Barcelona, Barcelona, Spain
[4]Department of Ophthalmology, University of Utah School of Medicine, Salt Lake City
[5]Departments of Neurobiology, Jules Stein Eye Institute and Brain Research Institute, University of California Los Angeles, Los Angeles
[6]Department of BioEngineering, University of Illinois at Chicago, Chicago
[7]Howard Hughes Medical Institute, University of California San Francisco, San Francisco

(RECEIVED January 9, 2004; ACCEPTED June 8, 2004)

Abstract

In the juvenile trkB knockout ($trkB^{-/-}$) mouse, retina synaptic communication from rods to bipolar cells is severely compromised as evidenced by a complete absence of electroretinogram (ERG) *b*-wave, even though the inner retina appears anatomically normal (Rohrer et al., 1999). Since it is well known that the *b*-wave reflects light-dependent synaptic activation of ON bipolar cells *via* their metabotropic glutamate receptor, mGluR6, we sought to analyze the anatomical and functional integrity of the glutamatergic synapses at these and other bipolar cells in the $trkB^{-/-}$ mouse. Although rod bipolar cells from wild-type juvenile mice were determined to be immunopositive for trkB, postsynaptic metabotropic and ionotropic glutamate receptor-mediated pathways in ON and OFF bipolar cells were found to be functionally intact, based on patch electrode recordings, using brief applications ("puffs") of glutamate or its analog, 2-amino-4-phosphonobutyric acid (APB), a selective agonist for mGluR6 receptors. Ionotropic glutamate receptor function was assayed in OFF-cone bipolar and horizontal cells by applying exogenous glutamatergic agonists in the presence of the channel-permeant guanidinium analogue, 1-amino-4-guanidobutane (AGB). Electron-microscopic analysis revealed that the ribbon synapses between rods and postsynaptic rod bipolar and horizontal cells were formed at the appropriate age and appear to be structurally intact, and immunohistochemical analysis did not detect profound defects in the expression of excitatory amino acid transporters involved in glutamate clearance from the synaptic cleft. These data indicate that there does not appear to be evidence for postsynaptic deficits in glutamatergic signaling in the ON and OFF bipolar cells of mice lacking trkB.

Keywords: Patch clamp recording, Agmatine uptake, Electronmicroscopy, Synapse, Excitatory amino acid transporter

Introduction

Tyrosine Kinase (TrkB) receptors are a family of three closely related receptor tyrosine kinases, each of which is activated by one or more of the neurotrophins (Huang & Reichardt, 2003). The Trk receptors mediate most of the survival-promoting and differentiation-promoting actions of the four neurotrophins (Kaplan & Miller, 2000; Huang & Reichardt, 2001; Patapoutian & Reichardt, 2001; Hempstead, 2002). TrkB is strongly activated by brain-derived neurotrophic factor (BDNF) and neurotrophin 4 (NT-4) (Huang & Reichardt, 2003), and in some cells is also activated by NT-3. Both trkB and its ligands are expressed in the mouse retina where they regulate neuronal differentiation (Di Polo et al., 2000; Wahlin et al., 2001; Lom et al., 2002). BDNF and NT-3 are expressed in retinal ganglion and inner nuclear layer cells (Bennett et al., 1999; Cusato et al., 2002; Pollock & Frost, 2003), whereas trkB is widely expressed in the retina. Cell-specific labeling has been reported in dopaminergic amacrine, retinal ganglion, horizontal, and Müller glial cells (Cellerino & Kohler, 1997; Llamosas et al., 1997; Rohrer et al., 1999; Vecino et al., 2002).

Rod photoreceptor development is regulated by trkB-mediated signaling *in vivo* and in organ culture (Rohrer et al., 1999; Rohrer & Ogilvie, 2003). Using ERG recordings, we have shown that in *trkB* knockout mice, functional and structural development of rods lags in time relative to development in wild-type mice and up to 16 postnatal days (oldest time point studied; limited by animal's survival) there is no evidence of a functional synaptic connection between rods and rod bipolar cells. These findings are surprising

Address correspondence and reprint requests to: Baerbel Rohrer, Department of Ophthalmology, Medical University of South Carolina, 167 Ashley Avenue, Charleston, SC, 29425, USA. E-mail: rohrer@musc.edu

because rods do not express trkB receptors (Rickman & Brecha, 1995; Ugolini et al., 1995; Rohrer et al., 1999; Di Polo et al., 2000; Harada et al., 2000). Our findings, furthermore, suggest that rod (and possibly rod bipolar cell) development depends on remote-acting molecules controlled by trkB-receptor expressing cells. Indeed, recent experiments suggest that BDNF may modulate postnatal photoreceptor survival indirectly, by controlling the release of growth factors from Müller glia (Harada et al., 2002).

Our previous studies demonstrated that *trkB* knockout mice lack a detectable ERG *b*-wave at all ages tested (Rohrer et al., 1999). Since it is now widely accepted that the ERG *b*-wave is a direct electrical manifestation of rod bipolar cell activity (reviewed by Pugh et al., 1998), the collective *a*-wave and *b*-wave results imply that these mice suffer from a profound defect in the signaling pathway between rods and rod bipolar cells. The specific locus of the defect, whether presynaptic in the rod terminal, or postsynaptic in the rod bipolar cells, is not known, and cannot be investigated using ERG recordings.

The present study was undertaken with the objective of examining the anatomical and functional integrity of the glutamate synapse between photoreceptors and bipolar cells in $trkB^{-/-}$ mice. Although immunocytochemical studies demonstrated that trkB receptors are normally present on rod bipolar cells of wild-type (*wt*) mice, electrophysiological experiments and AGB mapping studies demonstrated that depolarizing (ON) and hyperpolarizing (OFF) bipolar cells from the $trkB^{-/-}$ retina respond to exogenous applications of glutamate analogs. Using electron microscopy (EM), no differences were observed in the ultrastructure of the rod ribbon synapse in $trkB^{-/-}$ mice when compared to *wt* mice, and immunocytochemical experiments failed to show profound differences in the expression of excitatory amino acid transporters, required for glutamate clearance. The absence of a profound defect in postsynaptic receptor-mediated signaling suggests that the trkB-dependent remote-acting molecules that control rod development do not mediate ribbon synapse morphology, or rod bipolar cell development and signaling.

Material and methods

Animals

The trkB knockout mouse line ($trkB^{-/-}$; Rohrer et al., 1999) was generated by deletion of the first coding exon that is shared by all trkB isoforms, so it expresses neither the kinase nor the non-kinase isoforms of trkB. $TrkB^{-/-}$ homozygous mutants die within 3 weeks of birth. The original heterozygous founders of the $trkB^{-/-}$ mice (mixed 129 × C57/Bl6) were outcrossed into an ICR (Institute of Cancer Research) background for improved survival. Experiments were performed on littermates raised under cyclic light conditions (12 h light, 12 h dark) at the University of California San Francisco animal care facility. Genotyping utilized mouse tail DNA samples and PCR analyses. All experiments were in accordance with the Association for Research in Vision and Ophthalmology guidelines for animal research, using protocols approved by the UCSF Committee on Animal Research.

Patch-clamp recordings

Retinal slices were prepared from eyes of $trkB^{-/-}$ mice and *wt* littermates between the ages of P12 and P19. Cells included in this study had a mean "age" of P15.0 (*wt*) and P14.8 ($trkB^{-/-}$). Mice were deeply anesthetized with CO_2 and decapitated. The eyes were removed and dissected in oxygenated Ames medium [(Ames III & Nesbett, 1981); Sigma, St. Louis, MO]. The retina was removed from the sclera and retinal pigment epithelium, trimmed, and cut into two pieces. One piece of retina was transferred to a glass coverslip, ganglion cells-side-up, in a bead of medium. After gently sucking off excess medium, a dry filter (Millipore, Bedford, MA) was placed on top of the retina. The filter paper and adherent retina were then removed to a custom-made recording and slicing chamber, and sliced into ~150 μm-thick sections using a custom-made tissue slicer. Finally, several slices were transferred to slots in the recording portion of the chamber and rotated 90 deg to expose the retinal layers.

The recording chamber was placed on the fixed stage of an upright microscope (Zeiss Axioscop, Thornwood, NY) equipped with epifluorescence and Nomarski optics. Slices were perfused continuously (at ~1 ml/min) using a gravity-fed system, and maintained at 37°C by warming the chamber bottom and the inflowing perfusate (Cell MicroControls, Norfolk, VA). A manually operated Hamilton valve (Hamilton Co., Reno, NV) was used to select between Ames' solution or a calcium-free Locke's solution containing 2–6 mmol/l $CoCl_2$ to block endogenous neurotransmitter release. Perfusing the slices for about 30 min prior to recording helped remove damaged cells from the surface of the slice.

Cells were studied using conventional whole-cell recording techniques. Electrodes were typically filled with a Cs-gluconate-based solution (in mmol/l: 130 CsOH, 120 D-gluconic acid, 10 CsCl, 3 $MgCl_2$, 10 HEPES-$Na_{0.5}$, 15 glucose, 3 ATP-Na_2, 1 GTP-Na_3; pH 7.2). EGTA (5–10 mmol/l) was included in some experiments, and in some early experiments K-gluconate was used instead of Cs-gluconate. Lucifer yellow (0.02–0.04%) was usually included to label and identify cells using fluorescence, although filling was not always successful. Cells were held at a potential of approximately −40 mV. Signals were acquired with an Axopatch 1D amplifier (Axon Instruments, Union City, CA), filtered with a 4-pole Bessel anti-aliasing filter (Warner Instruments, Hamden, CT), and digitized using an Instrutech ITC-16 (Instrutech, Port Washington, NY) and Pulse Control software package (freeware developed and distributed by the Bookman Laboratory at the University of Miami, FL). Subsequent analysis was done using Igor (Wavemetrics, Oswego, OR).

Cell somas in the outer half of the inner nuclear layer (INL) were targeted for study. This would be expected to enrich the cell sample pool for ON bipolar to the exclusion of OFF bipolar and amacrine cells. Horizontal and Müller cells were easily identified by their large capacitance and were not included in the analysis. Several cells with obvious amacrine-like features (no dendrite, complex axonal arborization) were excluded from analysis, but incomplete labeling (particularly of processes) prevents us from ruling out the possibility that some amacrine cells were included in our sample.

A Picospritzer (General Valve, Fairfield, NJ) under computer control was used to pressure eject solutions (i.e. puff) onto the outer plexiform layer (OPL) through a glass pipette (2–4 μm diameter tip). Puff durations were 100–400 ms, and puff solutions consisted of glutamate (0.3 to 1 mmol/l) or L(+)-2-amino-4-phosphonobutyric acid (APB; 100 μmol/l) in a solution matching the extracellular solution. In a few experiments the recording electrode was used to gently "pull" a cell from the slice, and puffs were then applied to the isolated cell.

A small optical bench delivered light from a light-emitting diode (LED) source, through a glass fiber optic cable, and up through the microscope condenser to the slice. An adjustable aperture con-

jugate to the specimen controlled the size of the spot stimulus, always >200 μm diameter in these experiments. The intensity and timing of stimuli were computer controlled using the Pulse software, the ITC-16, and custom-built LED driver circuitry. LED intensity was controlled by modulating the driving current. A small portion of the LED light was used in a feedback circuit to maintain LED linearity. Stimuli were brief flashes, 10 ms in duration.

AGB mapping

WT and *trkB*$^{-/-}$ retinas were rapidly isolated, flat-mounted on pieces of nitrocellulose filter (5 μm pore size, Whatman) and incubated in oxygenated Ames medium at 35°C (95% O_2, 5% CO_2). After a short rest period (10 min), the medium was replaced with pre-warmed, oxygenated medium for 180 sec, in which 25 mmol/l of the Na^+ ions have been replaced with AGB (1-amino-4-guanidobutane) (Marc, 1999*b*). Experiments were performed in the presence or absence of 30 μmol/l kainic acid (KA) on the two eyes of each animal. After 30 min of incubation, reactions were stopped by fixation in Karnovsky's fixative (see electron microscopy section) and tissue was processed for epoxy resin embedding and immunohistochemical visualization (Marc, 1999*b*). Sections (250 μm) were deplasticized, probed with antibody at 20°C overnight (in 1% goat serum in 0.1 mol/l phosphate buffer, pH 7.4 and 0.05% thimerosal, GSPBT), followed by secondary antibody treatment (1 nm gold conjugated anti-rabbit IgG in 1% GSPBT) and silver intensification (0.11% silver nitrate and 0.5% hydroquinone in 0.2 mmol/l citrate buffer, pH 4.85; 4 min at 30°C). Primary antibodies used in this study were anti-AGB glutaraldehyde-linked protein (Marc et al., 1990) and anti-GABA IgG (Signature Immunologics Inc., Salt Lake City, UT).

Electron microscopy

Animals were deeply anesthetized with CO_2 and perfused transcardially with Karnovsky fixative (2% paraformaldehyde, 4% glutaraldehyde in phosphate-buffered saline; pH 7.4). The posterior portion of each eye was cut into quadrants, fixed additionally for 1 h with 1% osmium tetroxide (0.1 mol/l sodium phosphate buffer, pH 7.2), dehydrated, and embedded in Araldite 502 (Ciba Geigy, Basel, Switzerland). Ultrathin sections for electron microscopy were stained with uranium and lead salts. Sections from three mice per genotype were analyzed for overall morphology of the ribbon synapses.

Synaptic ribbon length was measured from digital images of ultrathin retinal sections taken from P16 *wt* and P16 *trkB*$^{-/-}$ mice. Two *wt* and two *trkB*$^{-/-}$ mice were included in the analysis. Synaptic ribbons in rod photoreceptor synaptic terminals that were sectioned at right angles to the plane of the ribbon were imaged with a KeenView digital camera (Soft Imaging System, Lakewood, CO) fitted to a Zeiss EM 910 electron microscope (Oberkochen, Germany). The microscope magnification was set at 10,000× for all of the images. The length of each ribbon was measured using analySIS™ software (Soft Imaging System, Lakewood, CO). A total of 40 synaptic ribbons were measured for the P16 *wt* retinas and 47 for the P16 *trkB*$^{-/-}$ retinas. Means and standard deviations from the mean were computed and the level of significance determined by the Student two-tailed *t*-test.

Immunohistochemistry

For immunohistochemistry on retinal sections, animals were decapitated, and eyes were enucleated and immersion-fixed in Carnoys fixative (10% acetic acid, 30% chloroform, 60% ethanol) for 2 h, after which they were dehydrated over several hours and embedded in paraffin in transverse orientation. Eyes were sectioned at 7 μm using a microtome and mounted on poly-L-lysine-coated slides. For retinal cell isolates, retinas from young *wt* mice (P14–P16) were isolated and incubated in papain medium (4.5 Units/ml, 37°C) for 30 min. After gentle trituration using a pasteur pipette, isolated cells were plated onto poly-D-lysine-coated coverslips, allowed to settle and attach for 30–45 min and fixed for 30 min in 4% paraformaldehyde.

Single antigens in tissue sections were visualized with horseradish peroxidase (HRP). Endogenous peroxidase was first quenched for 10 min in 3% hydrogen peroxide in Tris buffed saline (TBS) (100 mmol/l Tris-Cl, pH 7.5, 150 mmol/l NaCl) plus 10% methanol. Nonspecific binding was blocked by incubating sections for 1 h in blocking solution (3% bovine serum albumin, 10% normal goat serum and 0.4% Triton-X in TBS). Primary antibodies were applied overnight in blocking solution, followed by biotinylated secondary antibodies and the avidin and biotinylated horseradish peroxidase complex (ABC, Vector Laboratories Inc.; Burlingame, CA) for 1 h each. Slides were developed in DAB (0.05% diaminobenzidine in 0.1 mol/l Tris pH 7.5, and 0.003% hydrogen peroxide) for 1–5 min, dehydrated, and mounted in DPX. Sections were photographed using a Zeiss Axiophot, equipped with a digital camera and Spot acquisition software. For double-labeling immunohistochemistry, tissue sections or cells were first incubated in blocking solution for 1 h (see above), followed by the application of both primary antibodies which were raised in different species, for 4 h (single cells) or overnight (tissue sections). Antibody binding sites were visualized using fluorescently labeled secondary antibodies conjugated to Cy3 and Cy5 (Molecular Probes, Eugene, OR). Retinal sections were examined by confocal microscopy whereas single cells were photographed using a Zeiss Axiophot, equipped with fluorescence. Images were false-colored and superimposed using the Adobe® Photoshop software.

The following antibodies were used in this study: a rabbit polyclonal antibody against the extracellular domain of trkB (Meyer-Franke et al., 1998); a rabbit polyclonal against the kinase domain of trkB (a generous gift by D. Kaplan, University of Montreal; (Rohrer et al., 1999); a monoclonal antibody against PKCα/β (Amersham, Arlington Heigths, IL) to identify rod bipolar cells; and two polyclonal antibodies against the two main excitatory amino acid transporters in the retina: GLAST (a generous gift by M. Watanabe, Hokkaido University School of Medicine, Sapporo, Japan) and GLT-1 (a generous gift by J.D. Rothstein, Johns Hopkins University).

Real time PCR

Total RNA was isolated from P14 mice ($n = 4$ per genotype) using Trizol (Ambion, Austin, TX), followed by a clean-up with RNA-easy minicolumns (Quiagen, Valencia, CA). The quality of the RNA was examined by loading a small amount (1 μl) of sample on an agarose gel and visualizing the quantity and integrity of the 18s and 28s ribosomal RNA bands. Equal amounts of RNA were used in reverse-transcription reactions (Invitrogen, San Diego, CA) to generate complimentary DNA (cDNA) templates. PCR amplifications were conducted using the QuantiTect Syber Green PCR Kit (Quiagen) with 0.2 μmol/l forward and reverse primers and equal amounts of complimentary DNA (GLT-1: forward primer: TCT GAG GAG GCC AAT ACC AC; reverse primer: TTC ATC CCG TCC TTG AAC TC, amplicon size: 119 bp; GLAST: forward

primer: CCC ATC CCA GAG TCA GAA AA, reverse primer: CTC TTC TCC GTT GCT TTT GG, amplicon size: 142 bp; β-actin: forward primer: GCT ACA GCT TCA CCA CCA CA, reverse primer: TCT CCA GGG AGG AAG AGG AT, amplicon size: 123 bp). Real-time PCR were performed in triplicate in a GeneAmp® 5700 Sequence Detection System (Applied Biosystems, Foster City, CA) using the following cycling conditions: 50°C for 2 min, 94°C for 15 min, then 40 cycles of 94°C for 15 s and 58°C for 1 min. Quantitative values were obtained by the cycle number (C_t value), which is inversely proportional to the amount of a specific mRNA species. Relative gene expression levels were calculated using the equation $y = (1 + AE)^{\Delta\Delta C_t}$, where AE is the amplification efficiency of the target gene (set at 1.0 for all calculations), and $\Delta\Delta C_t$ the difference between the mean experimental and control ΔC_t values. The ΔC_t value is the difference between the C_t value for a retina-associated gene and the β-actin internal reference control gene. Data were expressed as mean ± standard error of the mean (SEM) and a Z-test was used to test for a difference from zero (i.e., no difference between *wt* and *trkb*$^{-/-}$ mice).

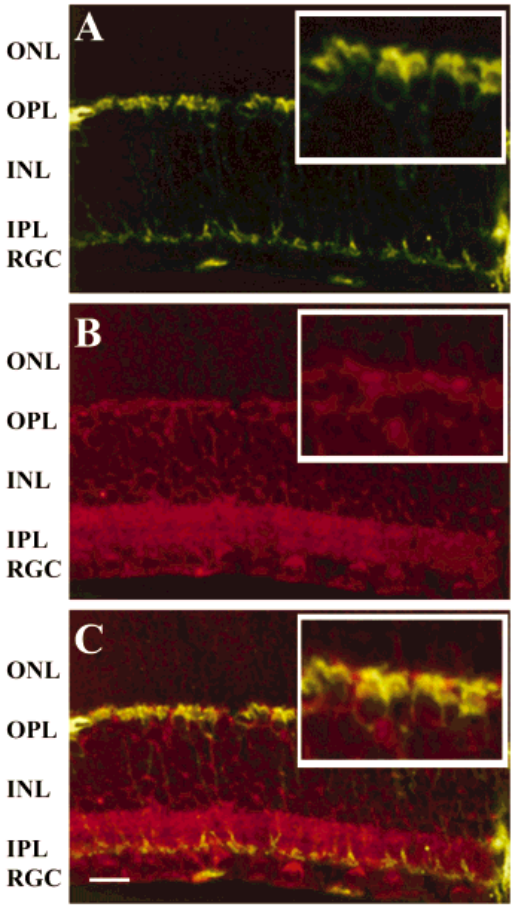

Fig. 1. Double-labeling immunohistochemistry using antibodies against PKCα/β (**A**) and TrkB (**B**) demonstrated that rod bipolar cells do express TrkB receptors (**C**). Scale for all panels is shown in Panel C = 10 μm. The insets focus on an identical section of the outer plexiform layer. ONL: outer nuclear layer; OPL: outer plexiform layer; INL: inner nuclear layer; IPL: inner plexiform layer; and RGC: retinal ganglion cells.

Results

Rod bipolar cells express TrkB receptors

We had shown previously that the distribution of TrkB receptors follows the development and maturation of the mouse retina (Rohrer et al., 1999). Here, using fluorescently labeled antibodies, TrkB was localized to cell bodies in the distal part of the outer nuclear layer as well as the outer plexiform layer of P14 *wt* retinas. Double-labeling immunohistochemistry for PKCα/β (Fig. 1A) and TrkB (Fig. 1B) revealed that rod bipolar cells account for some of the TrkB immunoreactivity in the inner nuclear layer and outer plexiform layer. Labeling of dissociated retinal cells obtained from P14–P16 *wt* retinas confirmed that all PKCα/β-positive cells were co-labeled with antibodies against TrkB (Fig. 2). It appears that rod bipolar cells grown in short-term cultures, like isolated retinal ganglion cells (Meyer-Franke et al., 1998), rapidly internalize TrkB receptors presumably due to the absence of appropriate external signals. Thus, out of the two cell types that make up the through-pathway for visual information processing, rod photoreceptors and rod bipolar cells, one is negative (i.e., rods), the other one is positive (i.e., rod bipolar cells) for the TrkB receptors.

Normal response to glutamate of postsynaptic metabotropic receptors

In normal mammals, the bipolar cells respond to the modulation of glutamate released by photoreceptor cells. Rod and cone ON bipolar cells possess mGluR6 glutamate receptors that mediate a

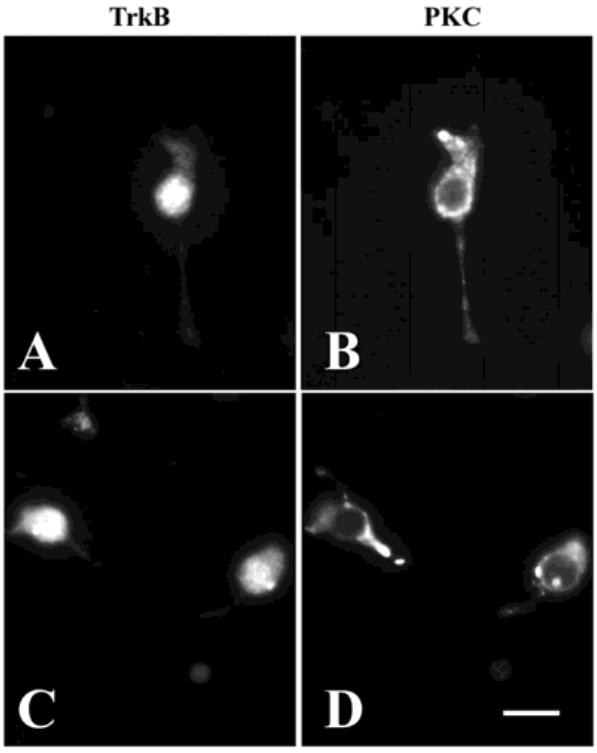

Fig. 2. Identification of TrkB (left-hand column) and PKCα/β (right-hand column) in isolated rod bipolar cells. Scale for all panels = 3 μm.

hyperpolarizing response to glutamate (Masu et al., 1995), whereas cone OFF bipolar cells possess ionotropic glutamate receptors (iGluRs) that lead to depolarizing responses. The absence of a recordable ERG *b*-wave in *trkb*$^{-/-}$ mice raises the possibility that bipolar cells, particularly rod ON bipolars, do not respond properly to glutamate. To test this idea, we made patch electrode recordings from bipolar cells in a retinal slice preparation and tested whether they responded to brief applications ("puffs") of glutamate or its analog APB, a selective agonist for mGluR6 receptors (Slaughter & Miller, 1985; Euler et al., 1996; McGillem & Dacheux, 2001).

In *wt* mice, 25 cells were studied. Based on responses to glutamate or APB puffs, nine of these were classified as ON bipolar and 11 were classified as OFF bipolar cells (Figs. 3B & 3D). Five were unresponsive to either APB (4 cells) or glutamate (1 cell). In *trkB*$^{-/-}$ mice, 22 of 44 cells tested responded to glutamate or APB with outward currents, and so were classified as ON-type bipolar cells (Fig. 3A). Seven cells, presumably OFF bipolar cells, responded to glutamate with inward currents (Fig. 3D). Fifteen cells were unresponsive, but most of these (10 of the 15) were tested only with APB, so some may have been OFF cells.

Strongest evidence for the integrity of the ON pathway comes from experiments using APB puffs, or glutamate puffs when synaptic transmission was blocked with Co^{2+} and 0 Ca^{2+} in the perfusate (Fig. 3A). Peak responses to 100 μmol/l APB were similar in *trkB*$^{-/-}$ and *wt* mice (12.6 ± 11.3 pA, $n = 8$, in *trkB*$^{-/-}$; 12.1 ± 19 pA, $n = 4$, in *wt*). ON responses to glutamate (0.8–1 mmol/l) were more variable (23 ± 32 pA, $n = 3$, in *trkB*$^{-/-}$; 15.5 ± 5.0 pA, $n = 2$, in *wt*). OFF-bipolar cells also gave similar peak responses (inward currents) to glutamate puffs (0.8–1 mmol/L) in *trkB*$^{-/-}$ and *wt* mice (−25 ± 25 pA, $n = 4$ in *trkB*$^{-/-}$; −34 ± 27 pA, $n = 9$ in *wt*).

A significant portion of putative rod bipolar cells in both *wt* and *trkB*$^{-/-}$ retinas did not respond vigorously to exogenous puffs of glutamate or APB. Euler and colleagues (Euler et al., 1996) similarly reported responses from only 50% of rod bipolar cells in their study using rat slices. In contrast, light-evoked (glutamate-mediated) responses from *wt* ON bipolar cells could be consistently recorded

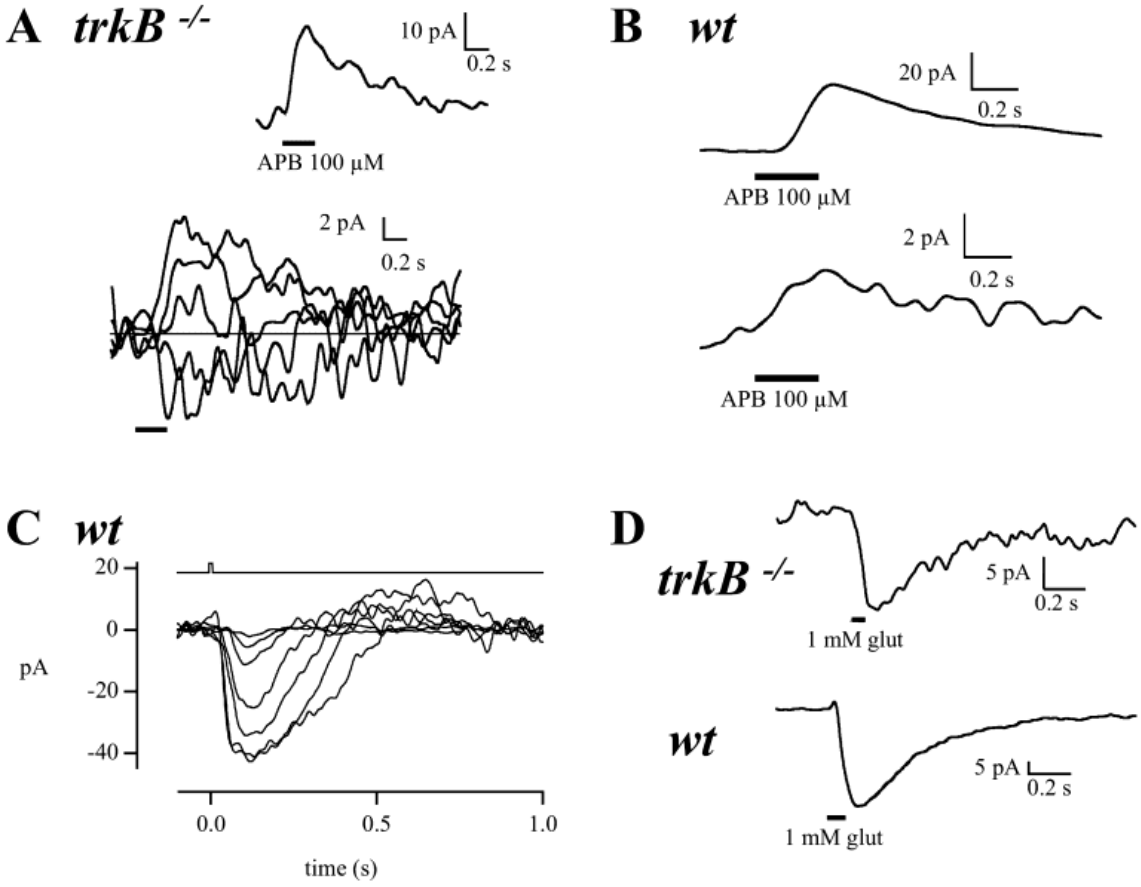

Fig. 3. Evoked currents (**A**) *trkB*$^{-/-}$. Responses from two different cells to puffs of 100 μmol/l APB. *Top*: Single trace, most likely from a cone ON bipolar cell, based on the location of its synaptic terminal. Perfusate contained 0 Ca^{2+} and 4 mmol/l $CoCl_2$ to block synaptic transmission. Age: P14. *Bottom*: ON bipolar cell, but the synaptic terminal was not labeled. Series of APB-evoked responses at different holding potentials. APB-evoked current reversed at ~0 mV. Age: P15. (**B**) *wt*: Responses from two different ON cells to puffs of 100 μmol/l APB. Age: P18 (*top*), P12 (*bottom*). (**C**) *wt*: Superimposed current responses of a rod bipolar cell to brief flashes of light delivering between 4 and 20,600 photons/μm^2 ($\lambda = 626$ nm). Timing of flash indicated by the uppermost trace. Age: P15. (**D**) *trkB*$^{-/-}$ (P14) and *wt* (P13). Responses of putative OFF bipolar cells to puffs of 1 mmol/l glutamate.

(Fig. 3C; D.M. Schneeweis and R.Blanco, unpublished observations, 2000). This difficulty with puffs is probably in part an access problem, since mGluR6 receptors are localized to the tips of ON bipolar dendritic processes that reside deep within the invaginating photoreceptor synapse. Furthermore, in mouse, light-evoked rod bipolar responses represent a summed input from ~20 rods (Tsukamoto et al., 2001), many below the surface of the slice, whereas exogenous puffs will be most effective close to the surface where the fragile dendritic terminals are most likely to be damaged. In contrast, $GABA_A$ and $GABA_C$ receptors are known to be more widely distributed over the cell surface of bipolar cells (Haverkamp & Wassle, 2000), and robust responses to GABA puffs were reliably obtained (data not shown).

In summary, we conclude that there does not appear to be a postsynaptic deficit in glutamatergic signaling in the bipolar cells of mice lacking trkB.

Normal responses to glutamate of postsynaptic ionotropic receptors

To look further into whether the ionotropic glutamate receptors that are present on mouse cone bipolar cells respond normally to glutamate in the *trkB* mutant retina, we examined the accumulation of AGB, a guanidinium analogue, which permeates open ionotropic glutamate-gated channels associated with α-amino-3-hydroxy-5-methylisoxazole-4-proprionic acid (AMPA), kainate, and N-methyl-d-aspartate (NMDA) receptors (Marc, 1999*b*). AGB is endogenously expressed at low levels in the mammalian brain (Li et al., 1994, 1995), where it is thought to act as a neuromodulator, but when applied exogenously in the presence of AGB-selective antiserum it is a useful tool for demonstrating the glutamatergic drive in the retina (Marc, 1999*b*).

Similar to previous observations on rabbit retina (Marc, 1999b), no endogenous AGB was detected in the mouse retina (B. Rohrer, unpublished observations, 2000). Acute (3 min) incubation of tissue in the presence of AGB alone (25 mmol/l) did not result in significant neuronal labeling in either the *wt* or the $trkB^{-/-}$ retinal tissue (Figs. 4A & 4C). However, following a 3-minute incubation in the presence of 100 μmol/l KA, a relatively specific agonist for AMPA and kainate receptors, a pattern of AGB labeling was observed in horizontal, bipolar, amacrine and ganglion cells that was indistinguishable between *wt* and $trkB^{-/-}$ retinas (Figs. 4B & 4D). The strength of the signal varied both between and within cell classes due to differences in receptor type and expression pattern (Marc & Jones, 2002). Kainate-induced labeling of Müller cells in *wt* and $trkB^{-/-}$ retinas is likely due to activation of glial stretch receptors (Marc, 1999*b*) following kainate-activated retinal swelling *in vitro*. Müller cells in rabbits and fish never show significant kainate-activated signals (Marc, 1999*a*,*b*; Marc & Jones, 2002), but they are structurally more robust *in vitro* than the fragile mouse retina.

In mouse, as in other mammals, cell bodies of the ON and OFF subtypes of bipolar cells are segregated to the distal and middle portions of the INL, respectively (Haverkamp & Wassle, 2000). AGB labeling did appear to be specific to OFF bipolar cells as might be expected since ON bipolar cells receive their primary input *via* metabatropic glutamate receptors. There have been reports that mammalian ON bipolar cells too, can possess iGluR subunits (Hughes, 1997; Vardi et al., 1998); however, see the report by Haverkamp et al. (2000) (Haverkamp et al., 2000). Regardless, the similar AGB labeling patterns in the $trkB^{-/-}$ and *wt* retinas, especially in the distal INL, are not consistent with a profound difference in ionotropic receptor-mediated glutamatergic signaling in cells postsynaptic to photoreceptors (i.e. bipolar and horizontal cells) in the $trkB^{-/-}$ mouse retina.

Morphological analysis of the rod-bipolar synapse

As the electrophysiological studies suggest that glutamatergic signaling is not impaired in ON or OFF bipolar cells, we also investigated the morphology of the rod-bipolar synapse in *trkB* knockout mice. The ribbon synapses that are formed between rods, rod bipolar cells and horizontal cells were compared in P16 *wt* and $trkB^{-/-}$ retinas (Fig. 5). Rod ribbon synapses are characterized by an electron-dense ribbon in the cytoplasm of the presynaptic process (arrows in Figs. 5B & 5F), and invaginating contacts made by a central rod bipolar cell dendrite (asterisks in Figs. 5B & 5F) and two lateral horizontal cell dendrites (arrowheads in Figs. 5B & 5F). Representative results presented in Fig. 5 depict examples of rod ribbon synapses found in the outer plexiform layer of P16 *wt* and $trkB^{-/-}$ retinas. We found no obvious structural deficits either presynaptically or postsynaptically in the $trkB^{-/-}$ ribbon synapse. In both control (*wt*) and $trkB^{-/-}$ synapses, there were (1) presynaptic ribbons, without any obvious reduction in number and size (see morphometry of ribbon lengths below); (2) synaptic vesicles along the ribbon as well as throughout the rod spherule, making up the reserve pool; (3) postsynaptic densities; and (4) the triads. The synapses between cones and cone bipolar cells also showed no defect in the $trkB^{-/-}$ mouse retina as judged by the same criteria (data not shown). The mean length for the *wt* and $trkB^{-/-}$ ribbons were similar and there was no statistical difference in average length ($P > 0.11$). Mean ribbon length was 0.46 μm $\pm$ 0.21 (n = 47) for the $trkB^{-/-}$ ribbons and 0.39 μm $\pm$ 0.16 (n = 40) for the *wt* ribbons. The standard deviations were relatively large due to the fact that synaptic ribbons are crescent-shaped structures and the measured "length" is a function of the position at which the section is taken through the crescent. The number of docked vesicles was not counted in these ribbons, because we reasoned that if the observed complete absence of synaptic signaling were due to an anatomical defect detectable at the EM level, it had to be a drastic, obvious effect such as the absence of docked vesicles.

Excitatory amino acid transporters in the OPL

Normal synaptic signaling depends critically on the efficient clearance of glutamate from the synaptic cleft. In the OPL, this may involve several excitatory amino acid transporters (Rauen et al., 1996), but GLAST (EAAT, EAAT1; expressed in Müller cells) and GLT-1 (EAAT2; expressed in ON bipolar cells) are thought to be the most important for proper photoreceptor-to-bipolar cell communication (Rauen et al., 1996; Harada et al., 1998). To address the idea that abnormal glutamate uptake might account for the $trkB^{-/-}$ deficit, we examined the expression of GLT-1 and GLAST in retina. Immunohistochemical studies showed comparable levels of GLAST labeling in *wt* and $trkB^{-/-}$ retinas (Fig. 6, top row), whereas GLT-1 labeling appeared reduced in the mutant retina (Fig. 6, bottom row). Using real-time PCR, the expression levels were quantified at the mRNA level, demonstrating that GLT-1 was reduced ~2-fold in samples derived from the $trkB^{-/-}$ retinas (P <0.001), whereas the levels of GLAST were indistinguishable between the two genotypes (P = 0.4) (Fig. 6E).

Discussion

The experiments described above were motivated by our previous dark-adapted ERG work, demonstrating that $trkB^{-/-}$ mice possess

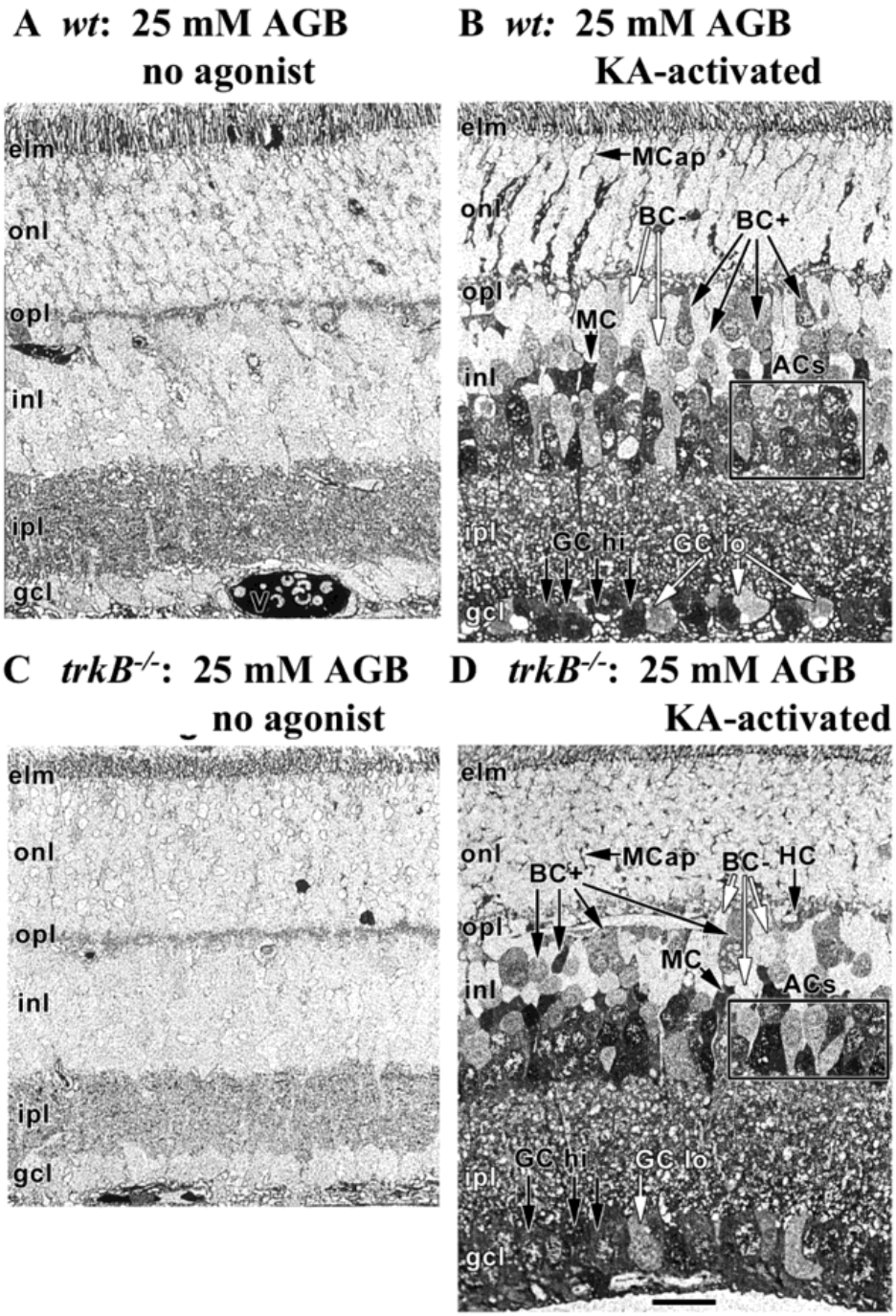

Fig. 4. AGB mapping in isolated wild type (*wt*; **A, B**) and *trkB*$^{-/-}$ (**C** & **D**) mouse retinas. Control retinas were probed with 25 mmol/l AGB (1-amino-4-guanidobutane) alone, while activated retinas were also exposed to 100 μmol/l kainate (KA). Background signals characteristic of the basal permeation of AGB through cation channels is evident in both *wt* (**A**) and *trkB*$^{-/-}$ retinas (**C**). Passive diffusion of AGB into cut vessels (V in Panel **A**) provides an internal calibration for presence of 25 mmol/l AGB. KA activation triggered massive AGB permeation into an array of neuron types known to express AMPA and/or KA receptors (**B** & **D**): *wt* and *trkB*$^{-/-}$ retinas are indistinguishable. Neurons varied in their strength of responses to KA, as described by Marc (Marc, 1999b) for rabbit retina. Clusters of amacrine cells (ACs, boxed in Panels **B** & **D**) range from high to moderate responsiveness in both *wt* and *trkB*$^{-/-}$ retinas. Similarly, strong (GC hi, black arrows, in Panels **B** & **D**) and weak (GC lo, white arrows, in Panels **B** & **D**) ganglion cell responses coexist in *wt* and *trkB*$^{-/-}$, as they do in the rabbit. Bipolar cell signals are more dramatically differentiated, being either clearly responsive (BC+, black arrows, probably OFF-center cells, in Panels **B** & **D**) or unresponsive (BC–, white arrows, probably ON-center cells, in Panels **B** & **D**). elm: external limiting membrane; gcl: ganglion cell layer; inl: inner nuclear layer; ipl: inner plexiform layer; onl: outer nuclear layer; and opl: outer plexiform layer. Scale for all panels (shown in Panel D) = 20 μm.

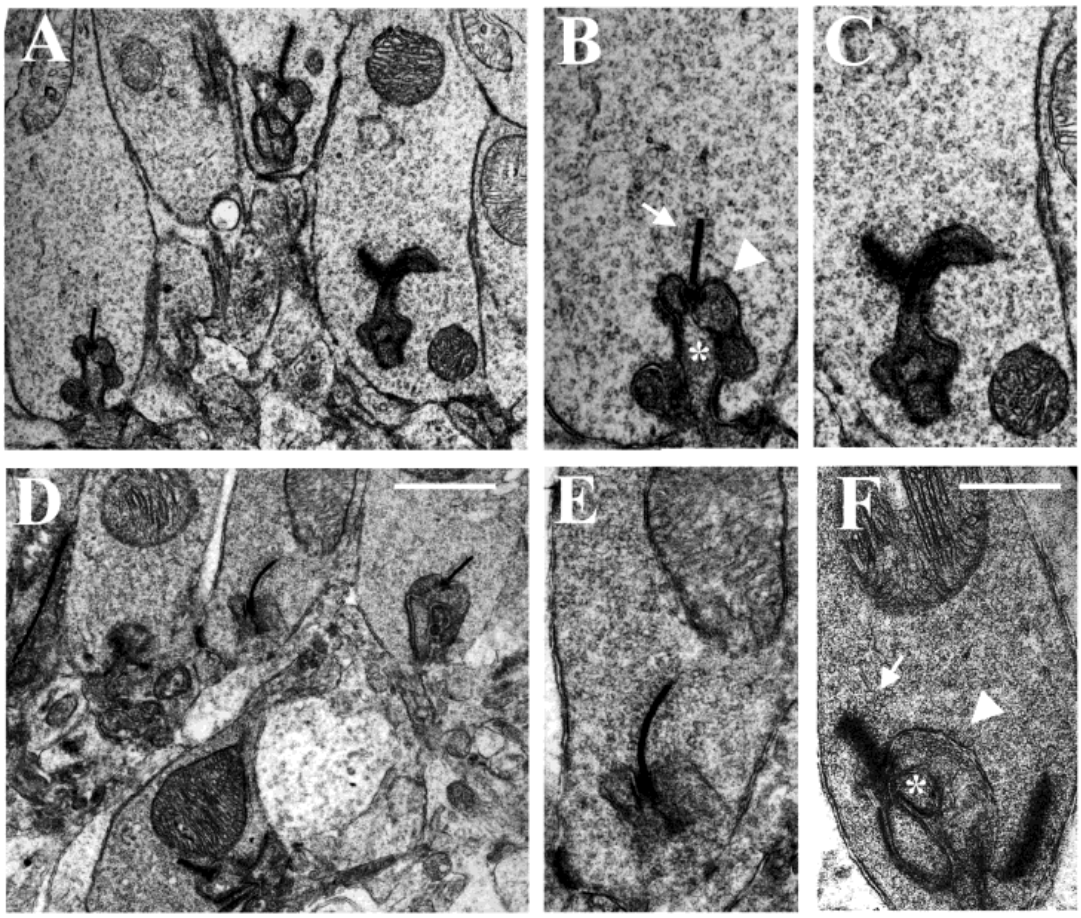

Fig. 5. Representative examples of ribbon synapses found in the outer plexiform layer in *wt* (**A–C**) and *trkB*$^{-/-}$ retinas (**D–F**). No obvious structural differences were found in the two genotypes based on four criteria: (1) normal number and size of presynaptic ribbons (arrows); (2) the presence of synaptic vesicles along the ribbon and throughout the rod spherule; (3) the presence of postsynaptic densities; and (4) the presence of triads (asterisks, rod bipolar cell dendrites; arrowheads, horizontal cell dendrites). Please note that rod pedicles in **C** and **E** were chosen to highlight the synaptic vesicles along the ribbons, whereas **B** and **F** were picked to illustrate the triad. Scalebar in Panel D for the overview images = 1 μm. Scale bar in Panel F for the details = 0.5 μm.

comparatively normal rod-mediated *a*-waves, but no *b*-waves, up to at least day P16, the approximate life expectancy of these mice (Rohrer et al., 1999). Since convincing data from several mammalian species now supports the hypothesis that the dark-adapted *b*-wave is generated by rod bipolar cells (Robson & Frishman, 1995, Green & Kapousta-Bruneau, 1999; Karwoski & Xu, 1999; Lei & Perlman, 1999), our observations indicate that a functional defect exists in the rod bipolar cell signaling pathway at some point proximal to the locus of phototransduction in the rods. The present study pursues this point further. Based on our finding that rod bipolar cells express trkB receptors, we carefully examined the integrity of the signaling pathway postsynaptic to the photoreceptor-bipolar cell synapse. Using multiple techniques to probe the glutamatergic drive, we demonstrated that postsynaptic bipolar cells can respond to exogenously applied glutamate. Additional experiments suggest that the nature of the *trkB*$^{-/-}$ defect is unrelated to obvious structural abnormalities of the rod ribbon synapse, and not due to a drastic downregulation of glutamate transporter expression around the photoreceptor synaptic terminal. We cannot, however, rule out the possibility that a combination of subtle effects involving the elements we investigated account for the *trkB*$^{-/-}$ phenotype.

Integrity of postsynaptic signaling pathways

Studies using transgenic or knockout mice have demonstrated that communication between rods and rod bipolar cells can be compromised by defects in any of several aspects of synaptic communication. Thus, defective glutamate release from rods (Ball et al., 2002), an absence of glutamate receptors on ON bipolars (Dhingra et al., 2002; Masu et al., 1995), and reduced glutamate re-uptake (Harada et al., 1998; Barnett & Pow, 2000) can all cause substantially reduced or altered *b*-wave. In this report, we focus on the postsynaptic and inner retina components. Our data indicate that deficits in postsynaptic neurons cannot explain the deficits observed in the *trkB*$^{-/-}$ mice. Of particular importance is our observation that ON bipolar cells responded to glutamate with outward currents of similar amplitude in both control and *trkB*$^{-/-}$ animals.

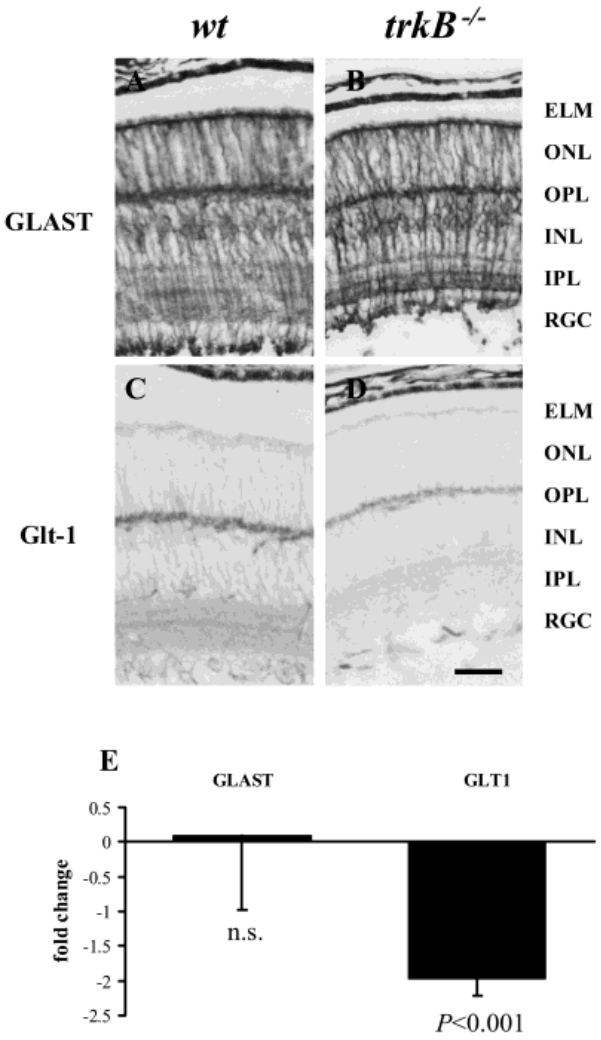

Fig. 6. Analysis of excitatory amino acid transporters at the protein (**A–D**) and mRNA level (**E**). Immunohistochemical profiles for excitatory amino acid transporters GLAST (**A** & **B**) and GLT-1 (**C** & **D**) in *wt* (left column) and *trkB*$^{-/-}$ retinas (right column). No difference in staining was observed with the GLAST antibody, whereas GLT-1 reactivity was reduced in the inner retina of the *trkB*$^{-/-}$ retina. Quantitative real-time PCR analysis confirmed the immunohistochemical observations (n = 5) (**E**). ELM: external limiting membrane; RGC: ganglion cell layer; INL: inner nuclear layer; IPL: inner plexiform layer; ONL: outer nuclear layer; and OPL: outer plexiform layer. Scale bar for all panels (shown in Panel D) = 20 μm.

In addition, ON bipolar cells appear to be present in normal numbers, and the mGluR6 receptors are localized to their dendritic terminals (Rohrer et al., 1999).

Our results also indicate that, in the *trkB*$^{-/-}$ mice, OFF bipolar cells, which are known to express ionotropic AMPA receptor subunits (Haverkamp et al., 2000; Haverkamp & Wassle, 2000), are able to respond normally to glutamate with inward currents of normal amplitude and kinetics. In addition, horizontal cells and OFF-cone bipolar cells were shown to accumulate AGB following glutamate application, indicating that the ionotropic glutamate receptors known to be present in these neurons were activated normally (Haverkamp et al., 2000; Haverkamp & Wassle, 2000). In summary, our results indicate that glutamate activates receptors normally in each of the cells in direct synaptic contact with photoreceptors. It is possible, however, that the glutamate receptors being activated by AGB, or by glutamate agonists in puff application experiments, are largely extrasynaptic. In that case, there would remain the possibility that the *trkB*$^{-/-}$ mouse has a defect in the postsynaptic localization of glutamate receptors. To answer this question would require immunogold localization of the glutamate receptor, which is beyond the scope of this study.

Anatomically intact ribbon synapses

The ERG deficit observed in the *trkB*$^{-/-}$ mouse is similar to, but more global than, that observed in the *mGluR6* knockout mouse (Rohrer et al., 1999). While ERGs of both knockout mouse genotypes are characterized by a lack of a recordable *b*-wave, *mGluR6*$^{-/-}$ mice showed immediate early gene expression in some cells in the inner retina in response to stroboscopic illumination [presumably activated through the OFF pathway (Yoshida et al., 1998)], whereas no such response was observed in the *trkB*$^{-/-}$ mice (Rohrer et al., 1999). These results need to be seen in the context of the data presented here, showing functional metabotropic and ionotropic glutamate receptors in the *trkB*$^{-/-}$ retina. The most parsimonious explanation would be that no functional synapses were formed in the outer plexiform layer to allow for synaptic transmission in these mice. Yet, our results show that the ribbon synapses between photoreceptor and bipolar cells form at the appropriate age and appear morphologically normal in EM. Direct testing of presynaptic photoreceptor function will be necessary to determine whether exocytosis or only light-mediated regulation of exocytosis is impaired. We are initiating experiments to examine regulated endocytosis and exocytosis, using FM1-43 in an effort to distinguish between these possibilities (Betz & Bewick, 1992; Kay et al., 1999).

A role for defects in glutamate transporters

As discussed above, synaptic transmission can also be compromised by defects in mechanisms responsible for the removal of neurotransmitter from the synaptic cleft (Harada et al., 1998). Mice deficient in GLAST, the major glial glutamate transporter in the retina, have a significantly reduced and slowed *b*-wave (Harada et al., 1998; Barnett & Pow, 2000), whereas elimination of GLT-1 only affected the onset kinetics of the *b*-wave, but not its amplitude (Harada et al., 1998). As the *b*-wave is triggered by the cessation of glutamate release from the photoreceptors in response to light, the slower kinetics of the *b*-wave indicate that regulation of glutamate removal from the synaptic cleft is defective, but not abolished in each of these mutants. As the dark-adapted *trkB*$^{-/-}$ ERG resembles an isolated PIII wave, without any indication of a *b*-wave (a much stronger phenotype than observed in the absence of either GLAST or GLT-1), it is very unlikely that a defect in glutamate transporters alone can be responsible for the lack of signaling in *trkB*$^{-/-}$ animals.

Possible mechanisms of neurotrophin action

Neurotrophin-mediated signaling has previously been shown to regulate both synapse development and function (e.g. Gonzalez et al., 1999; Huang et al., 1999; Alsina et al., 2001; Rico et al., 2002), exerting its effect through presynaptic or postsynaptic

signaling, depending upon the synapse (Kovalchuk et al., 2002; Zhang & Poo, 2002). In each of these examples, the effect on synapse development, maturation, or maintenance is presumably direct, because trkB is strongly expressed in at least one of the two cells that synapse with each other. In the case of the mouse ribbon synapse described here, the presynaptic cells (photoreceptors) express no or undetectable levels of trkB [(Rohrer et al., 1999) and Fig. 1], whereas the postsynaptic cells (rod bipolar cells) appear to express significant amounts of trkB receptors (Figs. 1 & 2); yet a bipolar cell defect could not be detected (Figs. 3–5).

At least two possible scenarios could account for the defect in synaptic communication observed in the *trkB*$^{-/-}$ mouse retina; first, a trkB-mediated retrograde signal derived from rod bipolar cells might control presynaptic signaling in the rod ribbon synapse; or second, the defect in synaptic signaling may instead reflect an indirect effect *via* remote-acting molecules, on the cells that form this synapse. In support of the first possibility, Micheva and colleagues (2003) have shown that the retrograde signaling molecule nitric oxide can regulate synaptic vesicle endocytosis and participate in synaptic vesicle recycling in hippocampal cells. In addition, nitric oxide (although maybe acting in a cell-autonomous way) has been shown to increase L-type Ca^{2+} channel-gating properties in salamander rod photoreceptors, providing a potential mechanism whereby the rod signal can be enhanced in postsynaptic neurons (Kurenny et al., 1994). These two mechanisms have not yet been addressed in the mouse retina. Alternatively, in previous studies, neurotrophins have been shown to regulate photoreceptor degeneration presumably through control of growth factor secretion from Müller glial cells (Harada et al., 2000).

To identify the cells through which trkB signaling controls synaptic communication in the retina will require cell-specific *trkB* deletions. Recently developed techniques, such as "caged BDNF" and temporally regulated gene deletion should also make it possible to eventually determine whether trkB regulates a developmental or a functional process at the photoreceptor-rod synapse (Kossel et al., 2001).

Acknowledgments

This work has been supported by grants from the National Institutes of Health (NS16033, EY13520, EY012100, EY00444, EY00331, EY014793, and EY02576). L. F. Reichardt is an Investigator of the Howard Hughes Medical Institute. D. Bok is the Dolly Green Professor of Ophthalmology at UCLA. R. Blanco was supported by grants from FIS 02/0926, and the Smith Kettlewell Eye Institute. Research was supported in part by an unrestricted grant to MUSC from Research to Prevent Blindness, New York, NY and a Center Grant from the Foundation Fighting Blindness to D. Bok. We thank Juan Korenbrot for constructive discussions, Heather Lohr, Priya Gogia, and Jane Hu for excellent technical assistance and Luanna Bartholomew for editorial assistance.

References

Alsina, B., Vu, T. & Cohen-Cory, S. (2001). Visualizing synapse formation in arborizing optic axons in vivo: dynamics and modulation by BDNF. *Nature Neuroscience* **4**, 1093–1101.

Ames, III, A. & Nesbett, F.B. (1981). *In vitro* retina as an experimental model of the central nervous system. *Journal of Neurochemistry* **37**, 867–877.

Ball, S.L., Powers, P.A., Shin, H.S., Morgans, C.W., Peachey, N.S. & Gregg, R.G. (2002). Role of the beta(2) subunit of voltage-dependent calcium channels in the retinal outer plexiform layer. *Investigative Ophthalmology and Visual Science* **43**, 1595–1603.

Barnett, N.L. & Pow, D.V. (2000). Antisense knockdown of GLAST, a glial glutamate transporter, compromises retinal function. *Investigative Ophthalmology and Visual Science* **41**, 585–591.

Bennett, J.L., Zeiler, S.R. & Jones, K.R. (1999). Patterned expression of BDNF and NT-3 in the retina and anterior segment of the developing mammalian eye. *Investigative Ophthalmology and Visual Science* **40**, 2996–3005.

Betz, W.J. & Bewick, G.S. (1992). Optical analysis of synaptic vesicle recycling at the frog neuromuscular junction. *Science* **255**, 200–203.

Cellerino, A. & Kohler, K. (1997). Brain-derived neurotrophic factor/neurotrophin-4 receptor TrkB is localized on ganglion cells and dopaminergic amacrine cells in the vertebrate retina. *Journal of Comparative Neurology* **386**, 149–160.

Cusato, K., Bosco, A., Linden, R. & Reese, B.E. (2002). Cell death in the inner nuclear layer of the retina is modulated by BDNF. *Brain Research Brain Research Reviews* **139**, 325–330.

Dhingra, A., Jiang, M., Wang, T.L., Lyubarsky, A., Savchenko, A., Bar-Yehuda, T., Sterling, P., Birnbaumer, L. & Vardi, N. (2002). Light response of retinal ON bipolar cells requires a specific splice variant of Galpha(o). *Journal of Neuroscience* **22**, 4878–4884.

Di Polo, A., Cheng, L., Bray, G.M. & Aguayo, A.J. (2000). Colocalization of TrkB and brain-derived neurotrophic factor proteins in green-red-sensitive cone outer segments. *Investigative Ophthalmology and Visual Science* **41**, 4014–4021.

Euler, T., Schneider, H. & Wassle, H. (1996). Glutamate responses of bipolar cells in a slice preparation of the rat retina. *Journal of Neuroscience* **16**, 2934–2944.

Gonzalez, M., Ruggiero, F.P., Chang, Q., Shi, Y.J., Rich, M.M., Kraner, S. & Balice-Gordon, R.J. (1999). Disruption of Trkb-mediated signaling induces disassembly of postsynaptic receptor clusters at neuromuscular junctions. *Neuron* **24**, 567–583.

Green, D.G. & Kapousta-Bruneau, N.V. (1999). A dissection of the electroretinogram from the isolated rat retina with microelectrodes and drugs. *Visual Neuroscience* **16**, 727–741.

Harada, T., Harada, C., Kohsaka, S., Wada, E., Yoshida, K., Ohno, S., Mamada, H., Tanaka, K., Parada, L.F. & Wada, K. (2002). Microglia-Muller glia cell interactions control neurotrophic factor production during light-induced retinal degeneration. *Journal of Neuroscience* **22**, 9228–9236.

Harada, T., Harada, C., Nakayama, N., Okuyama, S., Yoshida, K., Kohsaka, S., Matsuda, H. & Wada, K. (2000). Modification of glial-neuronal cell interactions prevents photoreceptor apoptosis during light-induced retinal degeneration. *Neuron* **26**, 533–541.

Harada, T., Harada, C., Watanabe, M., Inoue, Y., Sakagawa, T., Nakayama, N., Sasaki, S., Okuyama, S., Watase, K., Wada, K. & Tanaka, K. (1998). Functions of the two glutamate transporters GLAST and GLT-1 in the retina. *Proceedings of the National Academy of Sciences of the U.S.A.* **95**, 4663–4666.

Haverkamp, S., Grunert, U. & Wassle, H. (2000). The cone pedicle, a complex synapse in the retina. *Neuron* **27**, 85–95.

Haverkamp, S. & Wassle, H. (2000). Immunocytochemical analysis of the mouse retina. *Journal of Comparative Neurology* **424**, 1–23.

Hempstead, B.L. (2002). The many faces of p75NTR. *Current Opinion in Neurobiology* **12**, 260–267.

Huang, E.J. & Reichardt, L.F. (2001). Neurotrophins: Roles in neuronal development and function. *Annual Review of Biochemistry* **24**, 677–736.

Huang, E.J. & Reichardt, L.F. (2003). TRK receptors: Roles in neuronal signal transduction. *Annual Review of Biochemistry* **72**, 609–642.

Huang, Z.J., Kirkwood, A., Pizzorusso, T., Porciatti, V., Morales, B., Bear, M.F., Maffei, L. & Tonegawa, S. (1999). BDNF regulates the maturation of inhibition and the critical period of plasticity in mouse visual cortex. *Cell* **98**, 739–755.

Hughes, T.E. (1997). Are there ionotropic glutamate receptors on the rod bipolar cell of the mouse retina? *Visual Neuroscience* **14**, 103–109.

Kaplan, D.R. & Miller, F.D. (2000). Neurotrophin signal transduction in the nervous system. *Current Opinion in Neurobiology* **10**, 381–391.

Karwoski, C.J. & Xu, X. (1999). Current source-density analysis of light-evoked field potentials in rabbit retina. *Visual Neuroscience* **16**, 369–377.

Kay, A.R., Alfonso, A., Alford, S., Cline, H.T., Holgado, A.M., Sakmann, B., Snitsarev, V.A., Stricker, T.P., Takahashi, M. & Wu, L.U. (1999). Imaging synaptic activity in intact brain and slices with FM1-43 in C. elegans, lamprey, and rat. *Neuron* **24**, 809–817.

Kossel, A.H., Cambridge, S.B., Wagner, U. & Bonhoeffer, T. (2001). A caged Ab reveals an immediate/instructive effect of BDNF during hippocampal synaptic potentiation. *Proceedings of the National Academy of Sciences of the U.S.A.* **98**, 14702–14707.

Kovalchuk, Y., Hanse, E., Kafitz, K.W. & Konnerth, A. (2002). Postsynaptic induction of BDNF-mediated long-term potentiation. *Science* **295**, 1729–1734.

Kurenny, D.E., Moroz, L.L., Turner, R.W., Sharkey, K.A. & Barnes, S. (1994). Modulation of ion channels in rod photoreceptors by nitric oxide. *Neuron* **13**, 315–324.

Lei, B. & Perlman, I. (1999). The contributions of voltage- and time-dependent potassium conductances to the electroretinogram in rabbits. *Visual Neuroscience* **16**, 743–754.

Li, G., Regunathan, S., Barrow, C.J., Eshraghi, J., Cooper, R. & Reis, D.J. (1994). Agmatine: an endogenous clonidine-displacing substance in the brain. *Science* **263**, 966–969.

Li, G., Regunathan, S. & Reis, D.J. (1995). Agmatine is synthesized by a mitochondrial arginine decarboxylase in rat brain. *Annals of the New York Academy of Sciences* **763**, 325–329.

Llamosas, M.M., Cernuda-Cernuda, R., Huerta, J.J., Vega, J.A. & Garcia-Fernandez, J.M. (1997). Neurotrophin receptors expression in the developing mouse retina: An immunohistochemical study. *Anatomy and Embryology* **195**, 337–344.

Lom, B., Cogen, J., Sanchez, A.L., Vu, T. & Cohen-Cory, S. (2002). Local and target-derived brain-derived neurotrophic factor exert opposing effects on the dendritic arborization of retinal ganglion cells in vivo. *Journal of Neuroscience* **22**, 7639–7649.

Marc, R.E. (1999*a*). Kainate activation of horizontal, bipolar, amacrine, and ganglion cells in the rabbit retina. *Journal of Comparative Neurology* **407**, 65–76.

Marc, R.E. (1999*b*). Mapping glutamatergic drive in the vertebrate retina with a channel- permeant organic cation. *Journal of Comparative Neurology* **407**, 47–64.

Marc, R.E. & Jones, B.W. (2002). Molecular phenotyping of retinal ganglion cells. *Journal of Neuroscience* **22**, 413–427.

Marc, R.E., Liu, W.L., Kalloniatis, M., Raiguel, S.F. & van Haesendonck, E. (1990). Patterns of glutamate immunoreactivity in the goldfish retina. *Journal of Neuroscience* **10**, 4006–4034.

Masu, M., Iwakabe, H., Tagawa, Y., Miyoshi, T., Yamashita, M., Fukuda, Y., Sasaki, H., Hiroi, K., Nakamura, Y., Shigemoto, R. & et al. (1995). Specific deficit of the ON response in visual transmission by targeted disruption of the mGluR6 gene. *Cell* **80**, 757–765.

McGillem, G.S. & Dacheux, R.F. (2001). Rabbit cone bipolar cells: Correlation of their morphologies with whole-cell recordings. *Visual Neuroscience* **18**, 675–685.

Meyer-Franke, A., Wilkinson, G.A., Kruttgen, A., Hu, M., Munro, E., Hanson, J.M.G., Reichardt, L.F. & Barres, B.A. (1998). Depolarization and cAMP elevation rapidly recruit TrkB to the plasma membrane of CNS neurons. *Neuron* **21**, 681–693.

Micheva, K.D., Buchanan, J., Holz, R.W. & Smith, S.J. (2003). Retrograde regulation of synaptic vesicle endocytosis and recycling. *Nature Neuroscience* **6**, 925–932.

Patapoutian, A. & Reichardt, L.F. (2001). Trk receptors: Mediators of neurotrophin action. *Current Opinion in Neurobiology* **11**, 272–280.

Pollock, G.S. & Frost, D.O. (2003). Complexity in the modulation of neurotrophic factor mRNA expression by early visual experience. *Brain Research Brain Research Reviews* **143**, 225–232.

Pugh, Jr., E.N., Falsini, B. & Lyubarsky, A.L. (1998). The origin of the major rod- and cone-driven components of the rodent electroretinogram and the effect of age and light-rearing history on the magnitude of these components. In *Photostasis and Related Phenomena*, ed. Williams, T.P. & Thistle, A.B. pp. 93–128. New York: Plenum Press.

Rauen, T., Rothstein, J.D. & Wassle, H. (1996). Differential expression of three glutamate transporter subtypes in the rat retina. *Cell Tissue Research* **286**, 325–336.

Rickman, D.W. & Brecha, N.C. (1995). Expression of the proto-oncogene, trk, receptors in the developing rat retina. *Visual Neuroscience* **12**, 215–222.

Rico, B., Xu, B. & Reichardt, L.F. (2002). TrkB receptor signaling is required for establishment of GABAergic synapses in the cerebellum. *Nature Neuroscience* **5**, 225–233.

Robson, J.G. & Frishman, L.J. (1995). Response linearity and kinetics of the cat retina: The bipolar cell component of the dark-adapted electroretinogram. *Visual Neuroscience* **12**, 837–850.

Rohrer, B., Korenbrot, J.I., La Vail M.M., Reichardt, L.F. & Xu, B. (1999). Role of neurotrophin receptor TrkB in the maturation of rod photoreceptors and establishment of synaptic transmission to the inner retina. *Journal of Neuroscience* **19**, 8919–8930.

Rohrer, B. & Ogilvie, J.M. (2003). Retarded outer segment development in TrkB knockout mouse retina organ culture. *Molecular Vision* **9**, 18–23.

Slaughter, M.M. & Miller, R.F. (1985). Characterization of an extended glutamate receptor of the on bipolar neuron in the vertebrate retina. *Journal of Neuroscience* **5**, 224–233.

Tsukamoto, Y., Morigiwa, K., Ueda, M. & Sterling, P. (2001). Microcircuits for night vision in mouse retina. *Journal of Neuroscience* **21**, 8616–8623.

Ugolini, G., Cremisi, F. & Maffei, L. (1995). TrkA, TrkB and p75 mRNA expression is developmentally regulated in the rat retina. *Brain Research* **704**, 121–124.

Vardi, N., Morigiwa, K., Wang, T.L., Shi, Y.J. & Sterling, P. (1998). Neurochemistry of the mammalian cone 'synaptic complex'. *Vision Research* **38**, 1359–1369.

Vecino, E., Garcia-Grespo, D., Garcia, M., Martinez-Millan, L., Sharma, S.C. & Carrascal, E. (2002). Rat retinal ganglion cells co-express brain derived neurotrophic factor (BDNF) and its receptor TrkB. *Vision Research* **42**, 151–157.

Wahlin, K.J., Adler, R., Zack, D.J. & Campochiaro, P.A. (2001). Neurotrophic signaling in normal and degenerating rodent retinas. *Experimental Eye Research* **73**, 693–701.

Yoshida, K., Imaki, J., Okamoto, Y., Iwakabe, H., Fujisawa, H., Matsuda, A., Nakanisi, S., Matsuda, H. & Hagiwara, M. (1998). CREB-induced transcriptional activation depends on mGluR6 in rod bipolar cells. *Brain Research Molecular Brain Research* **57**, 241–247.

Zhang, X. & Poo, M.M. (2002). Localized synaptic potentiation by BDNF requires local protein synthesis in the developing axon. *Neuron* **36**, 675–688.